

Collective and local molecular dynamics in the lyotropic mesophases of decylammonium chloride: ^1H and ^2H NMR study

Marcin Wachowicz and Stefan Jurga*

Institute of Physics, A. Mickiewicz University, Umultowska 85, 61-614 Poznań, Poland

Marija Vilfan

Jozef Stefan Institute, Jamova 39, 1000 Ljubljana, Slovenia

(Received 10 September 2003; revised manuscript received 17 June 2004; published 14 September 2004)

The collective and individual dynamics of decylammonium chloride (DACl) molecules in water environment were investigated as a function of surfactant concentration and temperature. In the presence of water the DACl forms a variety of self-assembled structures, ranging from isotropic micellar systems to lyotropic liquid crystalline phases of hexagonal, nematic, and lamellar types. In order to characterize the complex molecular dynamics that occur in the DACl-water system, we applied ^1H and ^2H NMR techniques that cover the whole frequency range between 1 kHz and 30 MHz. The slow molecular dynamics were studied by ^1H NMR fast-field-cycling T_1 measurements and pulse-frequency dependence of ^2H NMR transverse relaxation time, performed by means of the Carr-Purcell-Meiboom-Gill sequence. We detected a well-expressed contribution of order director fluctuations, i.e., layer undulations, with characteristic ω_L^{-1} frequency dependence of T_1^{-1} in the lamellar phase. Its presence indicates a relatively weak impact of interactions between neighboring DACl layers. The frequency dependence of proton T_1^{-1} in the hexagonal phase exhibits a different type of frequency dispersion, $T_1^{-1} \sim \omega_L^{-1.32}$. The increase in the exponent is explained with the quasi-one-dimensional character of fluctuations in elongated cylinders. Further, the T_1 and T_2 relaxation times of deuterons selectively attached to the C2 and C7 segments of the hydrocarbon chains of DACl were measured at a Larmor frequency of 30.7 MHz, providing quantitative information about local molecular dynamics.

DOI: 10.1103/PhysRevE.70.031701

PACS number(s): 61.30.Gd, 64.70.Md

I. INTRODUCTION

Decylammonium chloride— $\text{C}_{10}\text{H}_{21}(\text{NH}_3)^+\text{Cl}^-$ (DACl)—belongs to a family of long-chain cationic surfactants, considered to be model systems for biological membranes, emulsifiers, and detergents. In the presence of water the surfactant molecules self-assemble as the result of hydrophobic-hydrophilic interactions [1,2]. Various types of aggregates are formed depending on surfactant to solvent ratio, temperature and other agents (i.e., salt addition). In the first stages of aggregation the micelles are formed. However, for higher DACl concentrations other mesophases are created, namely hexagonal (molecules self-assembled into tubes), nematic (disklike micelles), and lamellar (bilayers). In the phase diagram of the DACl-water system the liquid crystalline phases do not follow in the usual order of appearance—the hexagonal phase area is namely surrounded on all sides by the isotropic phases [1,3]. Besides, the nematic phase appears in a narrow temperature range also in the binary system in contrast to the usual ternary system (DACl, ammonium chloride, H_2O).

In the earlier nuclear magnetic resonance (NMR) studies of DACl-water mesophases the ^2H and ^{17}O NMR line shapes, and spin-lattice relaxation times of water molecules, were analyzed in order to elucidate the dynamics of water molecules interacting with surfactant aggregates [4–6]. Fujiwara *et al.* used ^{35}Cl and ^2H NMR line-shape analysis of

selectively deuterated DACl molecules in systems with ternary composition (DACl, ammonium chloride, D_2O) to obtain information on the degree of order of lamellar and hexagonal mesophases upon cholesterol addition [7]. The multifield ^{13}C and ^2H NMR studies of spin-lattice relaxation times measured in the conventional MHz frequency regime and complemented with transverse spin relaxation measurements focused mainly on the micellar isotropic DACl phases [8,9], like previous experiments reported for similar surfactant systems [10,11]. The variety of molecular motions in the DACl-water system prompted us to carry out a comprehensive study of molecular dynamics in the expanded, 1 kHz–30 MHz, range by ^1H and ^2H NMR. The motions affecting the spin relaxation in the kHz frequency domain are usually collective molecular reorientations, i.e., director fluctuations, resulting from long-wavelength viscoelastic deformations. Since DACl forms the liquid-crystalline lamellar phase, we were particularly interested in collective out-of-plane layer fluctuations, known as undulations [12]. We have used several experiments to detect these motions, including the pulse-frequency dependence of ^2H NMR transverse relaxation time, T_2^{CP} , measured by means of the Carr-Purcell-Meiboom-Gill (CPMG) sequence [13], and ^1H NMR fast-field-cycling (FFC) T_1 measurements [14–17]. However, to obtain the full picture of molecular dynamics we have also studied the fast local motions by analyzing the temperature dependence of deuterium T_1 and T_2 relaxation times measured at 30 MHz as well as deuterium line shapes.

In Sec. II of this paper we present the preparation of materials and the experimental methods used in the present

*Electronic address: stjurga@amu.edu.pl

TABLE I. Transition temperatures determined for samples used in the studies. Assignment was made on basis of ^2H NMR line-shape analysis in the temperature range 285–365 K. Single spectral line observed on ^2H NMR spectra was indicative of isotropic phase.

Sample %	Phases and transition temperatures
49	~ 289 K ~ 293 K ~ 313 K
	lam+nem \rightarrow nem \rightarrow iso \rightarrow iso+hex
	~ 321 K ~ 345 K ~ 355 K
57	\rightarrow hex \rightarrow hex+iso \rightarrow iso
	~ 315 K ~ 355 K
	lam \rightarrow lam+iso \rightarrow iso
62	~ 320 K
	lam \rightarrow lam+iso

study. Section III discusses the theoretical background of the relaxometry studies and line-shape analyses. Section IV addresses mesophase characterization and field-dependent orientation. Experimental results related to the slow molecular dynamics in the kHz range are presented and discussed in Sec. V. Finally, fast molecular dynamics is addressed in Sec. VI.

II. MATERIALS AND METHODS

A. Sample preparation

Decylammonium chloride was prepared as described by Kertes [18]. The selectively deuterated $[2,2-d_2]$ and $[7,7-d_2]$ DACI was synthesized in a similar way as described by Jurga *et al.* [19]. The samples were prepared by adding either double-distilled light water or heavy water (Polatom, Otwock-Swierk) to a dry, solid DACI to achieve desired concentration. The samples containing deuterated DACI in H_2O were used for ^2H NMR, and those containing DACI in D_2O were used for ^1H NMR T_1 dispersion measurements. Experimental ^2H NMR investigation was focused on a series of samples with concentrations chosen to cover interesting regions of the phase diagram [1]. They contained as follows 49, 57, and 62 wt % of $[2,2-d_2]$ DACI in H_2O and 48, 57, and 62 wt % of $[7,7-d_2]$ DACI in H_2O . For ^1H NMR T_1 dispersion measurements the samples with similar concentrations of the DACI+ D_2O system were used. The various phases of these samples are presented in Table I. As shown later, they were identified through deuterium NMR spectra.

Both unoriented and macroscopically aligned samples were used for ^2H NMR experiments. To obtain the magnetically aligned lamellar phases the 57% samples were heated to 360 K (micellar isotropic phase) and allowed to cool in the probehead inside the magnet (4.7 T). Magnetic alignment of 62% lamellar samples was not possible due to too high lamellar-isotropic transition temperatures. The aligned hexagonal phase was obtained by heating the 48–49% samples in the magnetic field from the low-temperature isotropic phase to temperatures above isotropic-hexagonal transition. Alternatively, cooling the samples in the presence of magnetic field from high-temperature isotropic phase below hexagonal-isotropic transition temperature created alignment. An unoriented hexagonal phase was obtained by heating the 48–49% samples up to 325 K in the thermostatic

bath in zero magnetic field conditions (i.e., the terrestrial magnetic field) and transferring them immediately to the preheated probehead to perform NMR analysis.

B. Deuterium NMR

^2H NMR measurements were performed with a Bruker CXP spectrometer, equipped with a 4.7 T cryomagnet, operating at 30.7 MHz. The spectra were recorded using the quadrupolar echo sequence $(\pi/2)_x - \tau - (\pi/2)_y - \tau -$ in the temperature range from 283 to 368 K. The typical delay time (τ) was set to 10–20 μs . The $\pi/2$ pulse length was usually set between 2.2 and 3.0 μs . Typically, 128–1024 echo accumulations were used to improve the signal-to-noise ratio of resulting spectra. The temperature-dependent T_1 and T_2^{QE} relaxation times were measured using the inversion-recovery and quadrupolar echo sequences, respectively. The pulse-frequency-dependent deuteron transverse relaxation times (T_2^{CP}) were determined using the quadrupolar version of Carr-Purcell-Meiboom-Gill (CPMG) pulse sequence $(\pi/2)_x - \tau - [(\pi/2)_y - 2\tau]_n$ and only every second echo was detected [20]. The T_2^{CP} data are presented as a function of τ^{-1} .

C. Proton fast-field-cycling NMR

Proton spin-lattice relaxation times were measured using commercial fast-field-cycling NMR relaxometer (Stelar, Italy) operating in the Larmor frequency range from 6 kHz to 20 MHz [21,22]. For frequencies up to 4 MHz the cycling technique with pre-polarizing field (usually 10 MHz) was used, whereas for frequencies in the range 5–20 MHz the nonpolarizing cycling sequence was employed. The detection field was set to 8 MHz.

III. THEORETICAL BACKGROUND

A. Proton spin-lattice relaxation in the lamellar phase

In the case of protons, the spin relaxation is induced by the time-modulation of magnetic dipole-dipole interactions between neighboring spins. The relaxation rate is proportional to the combination of spectral density functions, which are Fourier transforms of autocorrelation functions of the fluctuating part of the dipolar Hamiltonian [23]. In the analysis of proton spin-lattice relaxation data in the lamellar phase we assume that at least two independent and superimposed processes cause the relaxation, namely collective order director fluctuations (ODF)—the collective motions of many molecules incorporated into the lamellar layer, and individual motions (IM's) [15]. Since these two processes are statistically independent, the total correlation function takes the following form:

$$G(t) = G_{\text{ODF}}(t)G_{\text{IM}}(t). \quad (1)$$

Taking into account that collective order director fluctuations are considerably slower than individual molecular motions, one can assume that $G_{\text{ODF}}(t) \sim G_{\text{ODF}}(0)$ on the time scale on which $G_{\text{IM}}(t)$ decays towards the residual correlation value $G_{\text{IM}}(\infty) = \text{const}$. According to Ref. [22], this leads to the following general formula for the total relaxation rate:

$$T_1^{-1} = T_{1(\text{ODF})}^{-1} + T_{1(\text{IM})}^{-1}, \quad (2)$$

where $T_{1(\text{ODF})}^{-1}$ and $T_{1(\text{IM})}^{-1}$ represent the effective contributions of the two processes, each modified by the presence of the other relaxation mechanism. The (IM) term is usually further divided into the contributions of molecular rotations and conformational changes (R) and of surface lateral diffusion modulating intermolecular dipolar spin-spin interactions (LD) [23–25]. The upper limit of Larmor frequencies available in our fast-field-cycling device was 20 MHz and our experiments did not include T_1 measurements with conventional spectrometers (frequencies higher than 20 MHz). Therefore we do not present a detailed study of individual molecular motions [8], but focus on the less known collective fluctuations of the molecular director.

In the lamellar phase, the orientation of molecular director \mathbf{n} is determined by the local normal to the bilayer. The local normal experiences reorientations due to the out-of-plane fluctuations of the bilayer, known as undulations. Such collective excitations preserve the thickness of the bilayer and the orientation of the DACI molecules remains parallel to the local normal. Although the spectrum of bilayer undulations extends over a wide dynamic range, the contribution of this relaxation mechanism to the total relaxation rate, $T_{1(\text{ODF})}^{-1}$, is the greatest at kHz frequencies, where it overwhelms the contribution of fast molecular motions. The undulations can be expressed in terms of overdamped plane waves with a continuous distribution of in-plane wave vectors q_\perp . The mean-square amplitude of the q_\perp th director mode is given by $\langle |\delta n(q_\perp)|^2 \rangle = (k_B T) / (K_1 l q_\perp^2)$ [12]. Here K_1 is the “splay” elastic constant of the bilayer and l its thickness. Due to a strong dissipation arising from the viscous damping by the surrounding water, the fluctuation modes are characterized by an exponential time decay with the decay constant $\tau(q_\perp) = \Gamma_{\text{lam}}^{-1} q_\perp^{-\chi}$. The coefficient Γ_{lam} depends on the viscoelastic properties of the system, and the exponent χ on the hydrodynamic model for planar wave damping. Marqusee *et al.* [26] demonstrated that the spin-lattice relaxation rate induced by bilayer undulations depends linearly on the inverse circular Larmor frequency ω_L in the same manner as had been evaluated for thermotropic liquid crystals with layered structure [27]. $T_{1(\text{ODF})}^{-1}$ is obtained as a sum, transformed into integral, of contributions of all excitation modes in the plane, i.e.,

$$T_{1(\text{ODF})}^{-1} \propto \int_0^\infty \frac{k_B T}{K_1 l q_\perp^2} \frac{\tau(q_\perp)}{[1 + \omega_L^2 \tau^2(q_\perp)]} q_\perp dq_\perp \propto \omega_L^{-1}. \quad (3)$$

In evaluating Eq. (3) only linear terms in the description of bilayer undulations have been taken into account and the lower and upper limits of the integral over q_\perp were extended from 0 to ∞ . In a real system the limits are determined by the lateral size of the layer and molecular size, respectively, limiting the linear dispersion regime of $T_{1(\text{ODF})}^{-1}$ to Larmor frequencies between ω_{\min} and ω_{\max} . Beyond these limits, the relaxation rate $T_{1(\text{ODF})}^{-1}$ is proportional to ω_L^{-2} for $\omega_L > \omega_{\max}$, whereas for $\omega_L < \omega_{\min}$ the dispersion curve levels off into a frequency independent “plateau.”

The linear frequency dependence of $T_{1(\text{ODF})}^{-1}$ induced by undulations of a bilayer is a direct consequence of the two-dimensional character of the system. The same “linear type” of $T_{1(\text{ODF})}^{-1}$ frequency dependence has been recently theoretically predicted and experimentally confirmed for quasi-spherical unilamellar lipid vesicles, where a discrete set of normal modes related to the shape fluctuations of the vesicle induces the relaxation [28,29]. It should be noted that the $T_{1(\text{ODF})}^{-1} \sim \omega_L^{-1}$ behavior for planar bilayers and vesicles appears regardless of the value of the exponent χ in the expression for $\tau(q_\perp)$ i.e., it is independent of the hydrodynamic model describing the damping of fluctuations modes [26,28]. On the other hand, the hydrodynamic model affects drastically the frequency ω_{\min} at which $T_{1(\text{ODF})}^{-1}$ levels off to assume a constant plateau value independent of ω_L .

A deviation from the linear dependence of $T_{1(\text{ODF})}^{-1}$ on the inverse Larmor frequency would take place if there are interactions among bilayers, characterized by the compressibility modulus B . They are expected at higher concentrations of DACI, where the spacing between bilayers decreases. Halle *et al.* demonstrated that, by taking into account the interactions between bilayers, a crossover from the linear dispersion regime into a logarithmic frequency dependence occurs. The crossover takes place at a frequency much higher than ω_{\min} [30,31]. In such a case, the $T_{1(\text{ODF})}^{-1} \sim \omega_L^{-1}$ behavior, characteristic of free bilayer undulations, would occur only in the MHz range, where it might be masked by fast molecular reorientations and hardly observable. In reality, it is difficult to estimate the conditions under which the undulations of bilayers in a stack would still appear as free, since this requires the knowledge of the compression modulus of the lamellar phase, which is extremely scarce.

Taking into account the undulations’ contribution to the relaxation rate in its simplest form [Eq. (3)], the equation used for fitting $T_1^{-1}(\nu)$ dependence to the experimental data is

$$T_1^{-1}(\nu) = A_{\text{ODF}} \nu^{-p} + A_{\text{IM}} f(\nu)_{\text{lam}} + C_{\text{IM}}, \quad (4)$$

where ν is the Larmor frequency, p is the exponent of the power law (expected to be 1 for the lamellar phase), and A_{ODF} , A_{IM} are constants related to the strengths of the relaxation mechanisms. $f(\nu)_{\text{lam}}$ is a dimensionless function describing the contribution to T_1^{-1} due to the time modulation of intermolecular dipolar interactions by molecular lateral diffusion in the layer [25]. A frequency dependent T_1^{-1} contribution in the frequency range between approximately 1 and 30 MHz might arise also from defect diffusion along the alkyl chain, which has the collective character in the frame of a single molecule [32]. The parameter C_{IM} accounts for individual molecular reorientations and the defect diffusion along the alkyl chain (conformational changes) if the fast motion limit condition has been fulfilled. However, presenting the measurements only up to 30 MHz, individual molecular motions cannot be discerned precisely and are not the primary issue of this work.

B. Proton spin-lattice relaxation in the hexagonal phase

The situation is different in the hexagonal phase which consists of mutually parallel cylindrical aggregates with ra-

dially oriented DACI molecules. The slow collective fluctuations in this phase might be bend fluctuations of the axis of the cylinder. Such thermal excitations can be expressed in terms of normal modes characterized by the one-dimensional wave vectors q_z , where z is the direction of the cylinder axis. Assuming through analogy with thermotropic liquid crystals that the time decay constant of q_z th mode is $\tau(q_z) = \Gamma_{\text{hex}1}^{-1} q_z^{-2}$, and that $\langle |\delta n(q_z)|^2 \rangle = (k_B T) / (K_3 A q_z^2)$ represents the mean-square amplitude of q_z th mode, the resulting spin-lattice relaxation rate is proportional to $\omega_L^{-3/2}$:

$$T_{1(\text{ODF})}^{-1} \propto \int_0^\infty \frac{k_B T}{AK_3 q_z^2 [1 + \omega_L^2 \tau^2(q_z)]} dq_z \propto \omega_L^{-3/2}. \quad (5)$$

K_3 denotes here the bending elastic modulus and A the cross section of the cylinder. In evaluating the above equation, the interactions among neighboring cylinders have been neglected and the limits of integration extended from 0 to ∞ for the sake of simplicity.

In contrast to the two-dimensional director fluctuations in the lamellar phase, where the resulting frequency dependence of $T_{1(\text{ODF})}^{-1}$ is basically independent of the exponent describing the relation $\tau(q_z)$, this point becomes crucial in the hexagonal phase. If $T_{1(\text{ODF})}^{-1}$ is calculated using $\tau(q_z) = \Gamma_{\text{hex}2}^{-1} q_z^{-3}$, i.e., using exponent -3 instead of -2 , which is more appropriate in view of the hydrodynamic interaction of cylinders with the surrounding medium [33], the resulting relaxation rate is proportional to $T_{1(\text{ODF})}^{-1} \sim \omega_L^{-4/3}$. Obviously, in the hexagonal phase the characteristic exponent of the $T_{1(\text{ODF})}^{-1}$ dispersion curve does not reflect only the dimensionality of the system but also the hydrodynamic model determining the damping time of fluctuations.

In cylindrical aggregates there is another relaxation mechanism which is not present in the lamellar phase. Because of the curved surface of the cylinder, translational diffusion of DACI molecules along this surface modulates not only intermolecular spin interactions as in the planar case but also intramolecular spin interactions, though in a slower time scale. The translational diffusion of molecules is here accompanied by the reorientation of long molecular axes [34,35]. The characteristic time for the diffusion-induced reorientation of molecules is $\tau_{\text{TR}} = R^2 / 4D_1$, where R is the radius of the cylinder and D_1 the translational diffusion constant in the direction of maximal curvature of the cylinder. For rough estimates one can use D_1 equal to the lateral diffusion constant D_{lat} in the lamellar phase. This mechanism, modulating primarily intramolecular dipolar interactions, is expected to prevail in the upper frequency range of the hexagonal phase. The fitted expression in the hexagonal phase is therefore

$$T_1^{-1}(\nu) = A_{\text{ODF}} \nu^{-p} + A_{\text{IM}} \left(\frac{\tau_{\text{TR}}}{1 + (2\pi\nu\tau_{\text{TR}})^2} + \frac{4\tau_{\text{TR}}}{1 + (4\pi\nu\tau_{\text{TR}})^2} \right). \quad (6)$$

So far, only the effect of director fluctuations on the spin-lattice relaxation rate T_1^{-1} has been discussed. It is important to note that equivalent information on the frequency dependence of the spin relaxation can be obtained from the transverse spin-relaxation rate T_2^{-1} . To attain this purpose, the de-

pendence of deuteron T_2^{-1} on the pulse spacing in the Carr-Purcell-Meiboom-Gill (CPMG) echo experiment should be measured [20]. In contrast to protons, the relaxation of deuteron spins is caused predominantly by their electric quadrupole interaction. The advantages of the CPMG method are the absence of the local magnetic-field effect at low frequencies and a better defined spin coupling constant, whereas a smaller frequency interval accessible to the measurements can be considered as a drawback.

C. C-D bond order parameter

From the quadrupolar splitting of ^2H NMR spectra, measured as frequency spacing of the spectral doublets recorded for aligned samples, or the spacing between the most intense lines ("horns") of the Pake's powder pattern in disordered samples, the C-D bond order parameters can be evaluated. The doublet spacing $\Delta\nu$ in the oriented samples depends additionally on the orientation of the average surface normal at a particular site with respect to the symmetry axis of the aggregate (angle α), on the orientation of the symmetry axis of the aggregate with respect to the magnetic field (angle β), and on the deviation (due to ODF) of the instantaneous surface normal from its average orientation (angle γ). For axially symmetric electric field gradient tensor, as in the case of the C-D bonds, the quadrupolar splitting is given by [34,36–38]

$$\Delta\nu_i = \frac{3}{2} \left(\frac{e^2 q Q}{h} \right) S_{\text{CD}}^{(i)} \left(\frac{3 \cos^2 \alpha - 1}{2} \right) \left(\frac{3 \cos^2 \beta - 1}{2} \right) \times \left(\frac{3 \cos^2 \gamma - 1}{2} \right), \quad (7)$$

where $e^2 q Q / h$ is the static quadrupole coupling constant, $S_{\text{CD}}^{(i)}$ is the carbon-deuterium bond order parameter relative to the local normal to the aggregate's surface, and index i denotes the chain segment number.

For the aligned lamellar phase, with layers' normal perpendicular to the magnetic field, $\alpha = 0^\circ$ and $\beta = 90^\circ$, Eq. (7) reduces to

$$\Delta\nu_i \approx \frac{3}{4} \left(\frac{e^2 q Q}{h} \right) S_{\text{CD}}^{(i)}. \quad (8)$$

The ODF factor has been here set equal to ≈ 1 as the amplitude of collective orientational fluctuations is relatively small compared to the large amplitude of local fluctuations of the C-D bond. If the lamellar sample is not oriented and there is an isotropic distribution of layer normals, the splitting of the two sharp peaks in the powder pattern has the same value [Eq. (8)]. Further, in the aligned hexagonal phase (of diamagnetically negative systems) the cylinder axes are approximately parallel to the magnetic field, therefore $\alpha = 90^\circ$ and $\beta = 0^\circ$. Obviously Eq. (8) describes again the magnitude of the quadrupole splitting in this case. However, in the non-oriented hexagonal phase, with an isotropic spatial distribution of cylinders' axes, the rotation of molecules around the cylinder axis reduces the splitting. The two sharp peaks in the powder pattern are now (with $\alpha = 90^\circ$ and $\beta = 90^\circ$) separated only by one-half of the splitting frequency of the

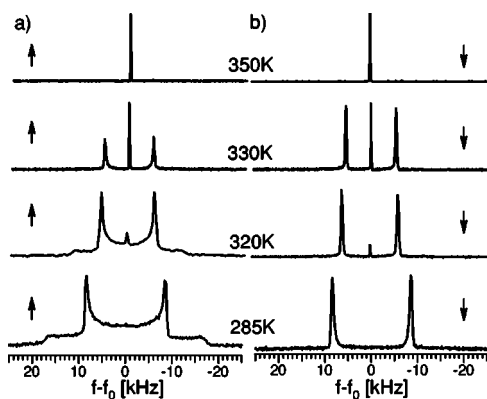


FIG. 1. ^2H NMR spectra of $[7,7-d_2]$ DACI 57% + H_2O system (a) with random distribution of director axes, recorded during heating, and (b) with domains aligned upon cooling in the magnetic field. Arrows indicate heating and cooling, respectively.

aligned hexagonal phase. Finally, in the isotropic phase consisting of micelles, the translational diffusion of molecules and micellar rotations average out the quadrupole interaction of deuterons to such an extent that only a single, narrow line appears in the spectrum.

IV. MAGNETIC ALIGNMENT MONITORED BY ^2H NMR SPECTROSCOPY

Before the relaxation experiments will be discussed, it is useful to analyze the ^2H NMR spectroscopic data obtained for the selectively deuterated DACI + H_2O binary system and especially those which relate to the magnetic alignment of DACI molecules. The reason for this is that without magnetic alignment of investigated samples some of the relaxation measurements presented in the next sections would be very difficult to perform due to the lower signal-to-noise ratio of spectra of unaligned samples.

The lamellar phase with isotropic distribution of director orientations, formed in the absence of magnetic field, gives a powder pattern on deuterium NMR spectrum as visualized in Fig. 1(a). When the sample is heated into the isotropic phase and then cooled down in the presence of magnetic field, the typical spectrum of the aligned lamellar system appears [Fig. 1(b)]. It consists of two narrow lines instead of the characteristic Pake's pattern, indicating that the average bilayer normals are aligned perpendicularly to the direction of the magnetic field. But all stacks of bilayers in the sample are still not necessarily parallel to each other. The sample might consist of domains of micrometer size with bilayers' normals spread in the plane perpendicular to the magnetic field. To unify the direction of all domains a stack of thin glassy plates should be used [2,39].

In Fig. 2 the ^2H NMR spectra of deuterium labeled DACI recorded as a function of temperature during transition from the lamellar to the nematic phase are presented. It is clearly seen that the domains of the lamellar phase are randomly spatially oriented whereas the nematic phase is uniformly aligned. The latter consists of discotic micelles and represents the intermediate stage between the lamellar and isotro-

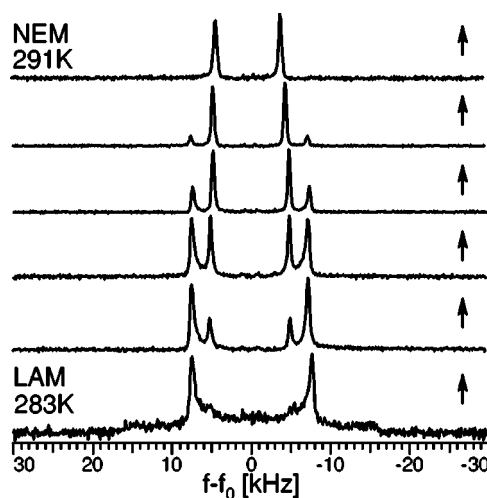


FIG. 2. ^2H NMR spectra recorded during the transition from lamellar to nematic phase in $[2,2-d_2]$ DACI 49% + H_2O system. Spectrum at the bottom corresponds to lamellar phase with random distribution of domains (powder pattern). Arrows indicate the rising of the temperature of the system.

pic phase. The quadrupole splitting in the spectra of the nematic phase is smaller than the splitting of the two peaks in the powder pattern of the lamellar phase. This fact reflects either the partial averaging of quadrupolar interaction on the edges of a discotic micelle or a smaller value of the C-D bond order parameter.

The selected ^2H NMR spectra of hexagonal phase with both disordered and aligned cylinders are shown in Fig. 3. According to the phase diagram, the hexagonal phase forms an island surrounded by the micellar isotropic phase. This peculiarity of the DACI-water system is clearly observed in Fig. 3(a). Upon heating the sample inside the magnet from the low-temperature isotropic phase, a spectral pattern of the hexagonal phase is obtained that corresponds to the cylinders aligned with their axes parallel to the direction of the magnetic field. At higher temperatures, the spectrum transforms

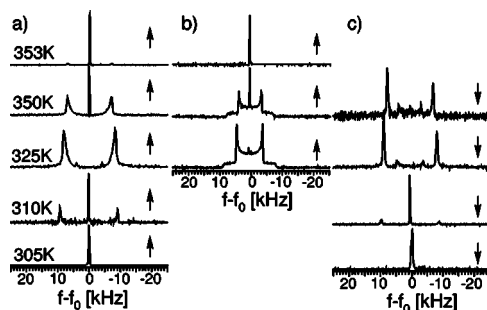


FIG. 3. ^2H NMR spectra of 48% $[7,7-d_2]$ DACI + H_2O system recorded as a function of temperature under three different experimental conditions: (a) with magnetic field applied during isotropic-hexagonal phase transition (magnetically aligned hexagonal phase); (b) the isotropic-hexagonal phase transition without applied magnetic field (random orientation of hexagonal cylinders); (c) cooling from high-temperature isotropic phase (partially aligned hexagonal phase). Arrows indicate the increasing and decreasing of the temperature.

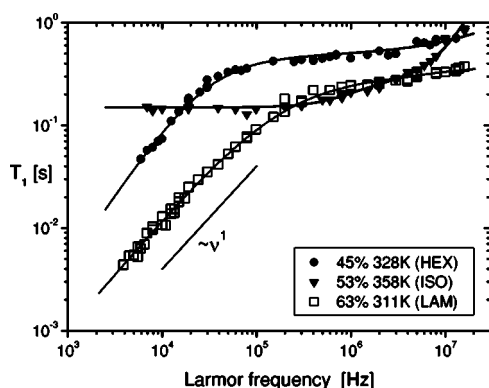


FIG. 4. Experimental frequency dependence of the proton spin lattice relaxation times in the hexagonal phase of 45% DACI/D₂O and in the lamellar phase of 53 and 63% DACI/D₂O systems. The results were fitted using functions given by Eqs. (4) and (6) and parameters listed in Table II.

again into a single line characteristic of the (high-temperature) isotropic phase. If the sample is heated to the hexagonal phase without applied magnetic field, a random distribution of cylinder orientations is obtained [Fig. 3(b)]. It was observed that the isotropic phase coexists with the hexagonal phase over the temperature range of at least several degrees. The spectra of coexisting phases consist of two components. The first one is a doublet or powder pattern with the splitting of the order of several kHz resulting from anisotropic motions of molecules forming cylinders. The second one is a single line resulting from random, isotropic motions of molecules forming micelles in the isotropic phase. These isotropic motions average the quadrupolar interaction to zero. Upon cooling the system from the high-temperature isotropic phase, the aligned hexagonal phase is also formed, but it is accompanied by considerable amount of randomly oriented domains contributing to residual powder pattern, superimposed on the doublet [Fig. 3(c)]. For faster temperature changes the more disordered system is created.

V. RESULTS AND DISCUSSION: SLOW COLLECTIVE MOTIONS

The frequency dependences of the proton spin-lattice relaxation times T_1 measured in the fast-field-cycling experiment for DACI+D₂O system are presented in Fig. 4 for the lamellar, hexagonal, and isotropic phases. It can be seen that the frequency dependence of T_1 in the high-temperature isotropic phase is limited to frequencies above 1 MHz, similarly as in the isotropic phase of thermotropic liquid crystals [23]. Below 1 MHz, T_1 in the micellar phase is frequency independent and indicates that micelles do not undergo collective orientational fluctuations with characteristic frequencies in the kHz range. The situation is different in the phases with larger and—in this system—anisotropic molecular aggregates. Both in the lamellar and in the hexagonal phases a strong frequency dispersion of the spin-lattice relaxation times appears below 100 kHz. It is expected to originate from the order director fluctuations (ODF) of DACI molecu-

TABLE II. Fitting parameters for T_1 FFC results for lamellar and hexagonal phases.

Sample	DACI 45%	DACI 63%
Phase	hex	lam
Temperature (K)	328	311
A_{ODF} (10^6) ^a	1.92	1.55
p	1.32	1.07
A_{IM} (10^8 s ⁻²) ^b	0.82	
A_{IM} (s ⁻¹) ^c		0.56
τ_{TR} (10^{-9} s)	4.83	
C_{IM} (s ⁻¹)		2.1

^aUnits depend on p .

^bParameter used in Eq. (6).

^cParameter used in Eq. (4).

lar aggregates. The experimental data for those two phases were therefore fitted using the models described by Eqs. (4) and (6). The values of the fitted parameters p , A_{ODF} , A_{IM} , C_{IM} , and τ_{TR} are given in Table II whereas the fixed value, $D_{lat} = 10^{-10}$ m²/s, was used for the lateral diffusion coefficient [8]. Notably, the best fit in the lamellar phase is obtained with the exponent $p \sim 1$, clearly showing the dominance of layer undulations in relaxing the spins below 100 kHz. A possible low-frequency plateau, which would be associated with the coherence length in the direction perpendicular to the bilayer surface, was not observed. The presence of the linear frequency T_1 dispersion in the kHz range indicates that the interactions among neighboring bilayers are not important in this frequency range. Obviously, those fluctuations modes which are here the most effective in the spin-relaxation process have the character of “free” undulations of a single bilayer. It might look different in samples with higher DACI concentration, where due to the lower water contents the interbilayer distance is smaller and interactions between neighboring bilayers may occur. The fitted value of A_{IM} in the lamellar phase is larger than it is usually in liquid crystals [25]. This fact suggests that the weak frequency-dependent contribution of T_1^{-1} in the MHz range arises not only from lateral molecular diffusion but possibly also from the conformational changes, described as the defect diffusion along the alkyl chain.

The proton T_1 frequency dependence measured in the hexagonal phase was fitted with Eq. (6). The fitted value of τ_{TR} is in good agreement with the calculated one according to $\tau_{TR} = R^2/4D_{lat}$. The evaluated exponent of the power law, $p = 1.32$, is not identical as in the lamellar phase, but agrees excellently with the value of $\frac{4}{3}$ predicted for ODF-induced relaxation in the hexagonal phase, where the fluctuations do not spread in the plane. They assume the quasi-one-dimensional character according to the shape of long cylindrical aggregates. The value of the exponent, close to $\frac{4}{3}$ and not 1.5, suggests that the dispersion relation for the mode relaxation time, $\tau(q_z)$, does not have the same dependence on the wave vector as in thermotropic liquid crystals. Obviously, the hydrodynamic interaction of cylinders with the surrounding medium affects the relaxation time of fluctuations in the

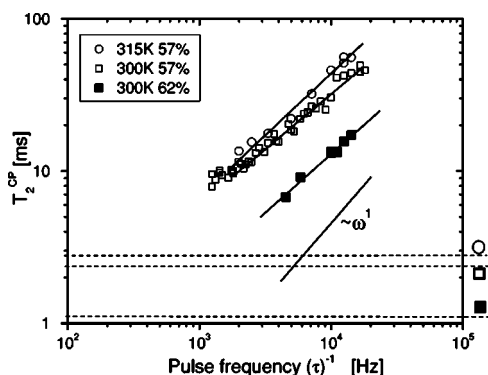


FIG. 5. Frequency dependent CPMG ^2H NMR spin-spin relaxation time measurements (empty symbols denote data from [7, 7- d_2] DACI 57% + H_2O system, filled squares show the results obtained at 300 K for [2,2- d_2] DACI 62% + H_2O). T_2^{OE} represents the limiting values which were measured using the quadrupolar echo sequence.

cylinders [33]. This effect could not be experimentally discerned in the lamellar phase where the linear frequency dependence of the spin relaxation rate appears irrespective of the dispersion relation for the relaxation time of overdamped fluctuation modes.

An interesting deviation from the above described ODF behavior is shown in Fig. 5 where the pulse frequency dependence of deuterium T_2^{CP} , measured with the CPMG pulse train experiment, is presented. The T_2^{CP} relaxation times were measured for magnetically aligned lamellar samples close to $\beta=90^\circ$. The average value of the exponent $p=0.76$ obtained from a power-law fitting is notably smaller than 1.0. The reason for this diminishing is that the transverse spin relaxation rate T_2^{-1} depends not only on the spectral density functions $J_1(\omega_L)$ and $J_2(2\omega_L)$, but also on $J_0(0)$ and has a totally different angular dependence than T_1^{-1} . For the sample normal oriented parallel or perpendicular to the magnetic field, the contribution of J_1 , which is the only spectral density function determined by the linear terms of the order fluctuations, reduces to zero. The relaxation is therefore induced by higher-order terms of order fluctuations which yield much weaker frequency dependence, i.e., p considerably smaller than 1 [40].

In similar way as in the case of proton T_1 dispersions we did not detect the low-frequency cutoff in $T_2^{\text{CP}}(\nu)$. However, the small value of the exponent p might partly originate from the vicinity of the frequency-independent plateau. The values of T_2^{OE} relaxation times obtained from quadrupolar echo spin-spin relaxation time measurements are plotted as horizontal lines in Fig. 5 and denote the asymptotic values $T_2^{\text{CP}}(\nu \rightarrow 0) = T_2^{\text{OE}}$.

The fact that different relaxation mechanisms are affecting T_2^{OE} and T_1 , though both relaxation times are measured at the Larmor frequency 30.7 MHz, is illustrated in Fig. 6. The measurements of the temperature dependence of T_2^{OE} and of T_1 reveal the difference between the contributions of fast molecular reorientations and of slow collective fluctuations in the lamellar phase. In contrast to the T_1 relaxation process which is mainly sensitive to spectral densities of motions at circular Larmor frequency $J_1(\omega_L)$ and twice the circular Lar-

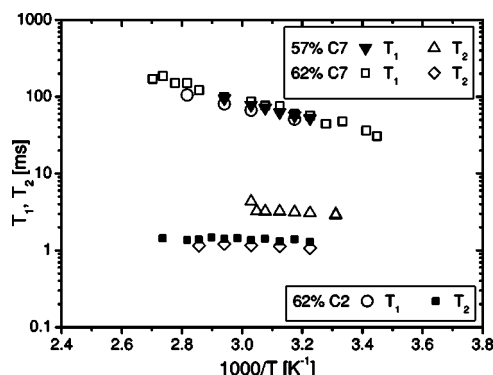


FIG. 6. Arrhenius plots of T_1 and T_2 ^2H NMR relaxation times measured for the lamellar phase of systems containing 62% DACI (with deuterated C2 or C7 segment) and 57% DACI (with deuterated C7) in H_2O .

mor frequency $J_2(2\omega_L)$ the T_2 relaxation time, though measured at the same Larmor frequency, is also affected by $J_0(0)$. In this way, it is sensitive also or even predominantly to much slower molecular reorientations, i.e., collective fluctuations of molecular aggregates. Figure 7 shows that T_2 values change considerably at the transition from hexagonal to micellar isotropic phase and also from lamellar to isotropic phase (data not shown), reflecting the changes of aggregate dynamics between micellar and liquid crystalline phases in the kHz frequency range. The values of T_1 are less affected by the transitions.

VI. RESULTS AND DISCUSSION: FAST LOCAL MOTIONS

A. Deuteron spin-lattice relaxation

The experimental deuteron T_1 results for the lamellar phase are shown in Fig. 6 for two different concentrations and deuteron positions. Obviously, the position of deuteron in the alkyl chain does not affect the T_1 values. This suggests that the spin-lattice relaxation at 30 MHz is induced mainly by the overall reorientations of molecules and to a smaller extent by the conformational changes. Molecular reorientations are so fast that the extreme narrowing limit takes place

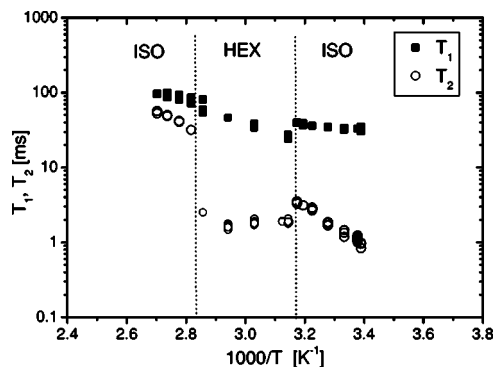


FIG. 7. Arrhenius plots of T_1 and T_2 ^2H NMR relaxation times of [2,2- d_2] DACI 49% + H_2O system. Discontinuity of relaxation times was observed at both isotropic-hexagonal and hexagonal-isotropic phase transitions.

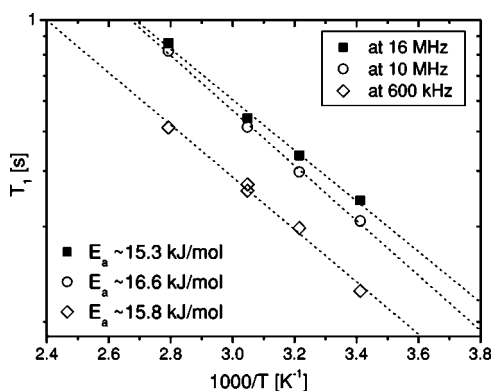


FIG. 8. Arrhenius plots of T_1 FFC ^1H NMR relaxation times of DACI 63% + D_2O system in the lamellar phase. The activation energies obtained from the slopes of high-temperature side of T_1 minimum are presented.

and only the high-temperature side of T_1 vs $1/T$ curve could be detected in the temperature range of the lamellar phase. The activation energies obtained from T_1 slopes of 62% system are 14.4 ± 0.4 and 15.5 ± 0.5 kJ/mol for DACI with deuterated C2 and C7 segments, respectively. Again, the activation energies are within the experimental error the same for the C2 and C7 deuteron positions. In Fig. 7 it is seen that at the isotropic-hexagonal and hexagonal-isotropic phase transitions the ^2H NMR T_1 relaxation time measurements at 30.7 MHz indicate a small discontinuity. The activation energies obtained from T_1 Arrhenius plots in the hexagonal phase are somewhat higher than the corresponding values obtained in the lamellar phase: 21.5 ± 1.2 and 22.8 ± 0.3 kJ/mol for 49% (C2) and 48% (C7) samples, respectively.

B. Proton spin-lattice relaxation dispersion

The contribution from fast molecular motions has been detected also in the proton T_1 relaxation. The T_1 values obtained from ^1H NMR fast-field-cycling measurements in 63% DACI + D_2O system at three Larmor frequencies ranging from 600 kHz up to 16 MHz are presented in Fig. 8. The calculated activation energies are almost the same as those obtained from deuterium T_1 measurements at 30.7 MHz. This corroborates the fact that the overall molecular reorientations and partly conformational changes are the important relaxation mechanisms in this frequency range and that the lateral diffusion plays a minor role.

C. C-D bond order parameters

The ^2H NMR spectra of selectively deuterated DACI molecules give information about fast anisotropic motions of particular C-D bonds. The quadrupolar splitting ($\Delta\nu$) for each of the C2 and C7 segment deuterons was measured in the lamellar phase at two DACI concentrations (57 and 62%) and the temperature dependence of the C-D bond order parameter, S_{CD} , evaluated on basis of Eq. (8), is presented in Fig. 9. The difference in the concentration of surfactant molecules is reflected in the S_{CD} values but the effect is smaller

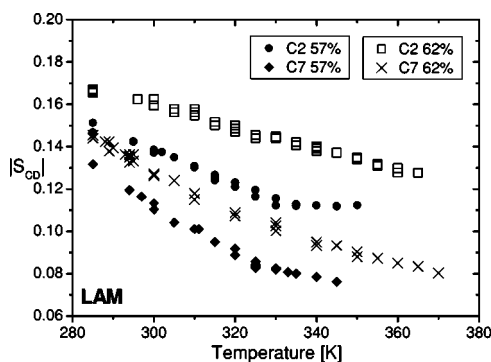


FIG. 9. Temperature dependence of order parameters for C2 and C7 segments of DACI in the system containing 57% and 62% DACI in H_2O (lamellar phase).

than 15%. The dependence of S_{CD} on the position in the alkyl chain is somewhat larger ($<30\%$). The smaller quadrupolar splitting and consequently the order parameter observed for C7 segment, with respect to this detected for C2 segment, reflects an increase in motional disorder along the chain. It is attributed to increased gauche conformation probability. The disorder progresses with the increase of temperature.

VII. CONCLUSIONS

In this paper a NMR relaxometry study of molecular dynamics in the DACI-water system is presented. It focuses on the slow, collective molecular dynamics in the lamellar and hexagonal phases. Two kinds of nuclei were used as the probe, protons and deuterons in selectively deuterated DACI compounds. In addition to the relaxometry studies, the mesophases were identified by using the deuterium NMR spectra, and the capability of the magnetic field to align these mesophases was examined.

We found that the application of a strong magnetic field during the formation of the lamellar and hexagonal phases on heating or cooling from the isotropic phases results in the alignment of molecular domains. The normal to the bilayers' stacks is perpendicular to the magnetic field in the oriented lamellar phase and the cylinders are parallel to the magnetic field in the ordered hexagonal phase. The ordering of the hexagonal phase is complete upon heating from the low-temperature isotropic phase, but only partial on cooling from the high-temperature isotropic phase. This indicates the dual character of the two isotropic phases in the DACI-water system. It was important to have oriented samples in the relaxometry studies; due to higher signal-to-noise ratio the experiments with oriented samples are not time consuming (not so many signal accumulations are required to obtain good quality spectra). This gave us an opportunity not only to acquire the spectra, but also to measure the deuteron T_1, T_2^{QE} relaxation times and T_2^{CP} frequency dependence.

The proton fast-field-cycling measurements of the spin-lattice relaxation time in the frequency range between 4 kHz and 20 MHz identified collective layer fluctuations, i.e., undulations, in the lamellar phase. They induce a specific, "linear" dependence of the spin-relaxation rate on the Larmor

frequency. Its very existence in the kHz range suggests that the interactions among bilayers in the DACI-water system are weak, that the compression modulus is small, and that the fluctuations inducing relaxation in this frequency range behave as “free” undulations of individual bilayers. This finding was confirmed by the deuteron T_2^{CP} results obtained from the CPMG experiment. The frequency dependence of the proton spin-lattice relaxation time measured in the hexagonal phase shows a different type of dispersion. The spin-lattice relaxation rate was found proportional to $\omega_L^{-1.32}$. We explained such behavior with the influence of bending motion of cylindrical aggregates, which is quasi-one-dimensional. Besides, in the case of one-dimensional fluctuations, the exponent of the T_1 dispersion discerns not only the dimensionality of fluctuations but also the way in which the relaxation time of fluctuations depends on the wave vector. We found that in the hexagonal phase of the system under study the damping of fluctuations by the surrounding water is essential, but that the fluctuations of cylinders are not hampered by mutual interactions.

The fast local motions influencing the ^2H NMR T_1 at high Larmor frequency were found to have similar character in all phases studied. The lack of the deuteron T_1 dependence on the position in the alkyl chain indicates that the relaxation is induced mainly by the overall reorientations of the molecule and to a smaller extent by its conformational changes. The analysis of the quadrupolar splitting gave us information on the order parameters of carbon-deuterium bonds at two different segments of the hydrocarbon chain of the molecule. We monitored the chain segments ordering as a function of temperature and surfactant concentration.

ACKNOWLEDGMENTS

The authors wish to thank Dr. M. Kempka for assistance in the measurements, Professor J. L. White for suggestions which helped to improve the manuscript, and Professor P. Sebastiao for the help in the fitting procedure. The financial support of KBN Grant No. 3 T09A 050 27 (M.W., S.J.), Kulczyk Family Fund (M.W.), and the Office of Science of Slovenia (M.V.) is gratefully acknowledged.

-
- [1] J. D. Gault, M. A. Leite, M. R. Rizzatti, and H. A. Gallardo, *J. Colloid Interface Sci.* **122**, 587 (1988).
- [2] M. C. Holmes and J. Charvolin, *J. Phys. Chem.* **88**, 810 (1984).
- [3] M. R. Rizzatti and J. D. Gault, *J. Colloid Interface Sci.* **110**, 258 (1986).
- [4] M. P. Frenot, H. Nery, and D. Canet, *J. Phys. Chem.* **88**, 2884 (1984).
- [5] L. Piculell, *J. Phys. Chem.* **89**, 3590 (1985).
- [6] M. P. Bozonnet-Frenot, J. P. Marchal, and D. Canet, *J. Phys. Chem.* **91**, 89 (1987).
- [7] F. Y. Fujiwara and L. W. Reeves, *J. Am. Chem. Soc.* **98**, 6790 (1976).
- [8] M. Törnblom, R. Sitnikov, and U. Henriksson, *J. Phys. Chem.* **104**, 1529 (2000).
- [9] H. Néry, O. Söderman, D. Canet, H. Walderhaug, and B. Lindman, *J. Phys. Chem.* **90**, 5802 (1986).
- [10] O. Söderman, U. Henriksson, and U. Olsson, *J. Phys. Chem.* **91**, 116 (1987).
- [11] I. Furó and B. Halle, *Phys. Rev. E* **51**, 466 (1995).
- [12] P. G. de Gennes and J. Prost, *The Physics of the Liquid Crystals* (Oxford University Press, Oxford, 1993).
- [13] G. Althoff, N. J. Heaton, G. Gröbner, R. S. Prosser, and G. Kothe, *Colloids Surf., A* **115**, 31 (1996).
- [14] R. Kimmich, *Bull. Magn. Reson.* **1**, 195 (1980).
- [15] E. Rommel, F. Noack, P. Meier, and G. Kothe, *J. Phys. Chem.* **92**, 2981 (1988).
- [16] J. Struppe, F. Noack, and G. Klose, *Z. Naturforsch., A: Phys. Sci.* **52a**, 681 (1997).
- [17] R.-O. Seitter, T. Link (Zavada), R. Kimmich, A. Kobelkov, P. Wolfangel, and K. Müller, *J. Chem. Phys.* **112**, 8715 (2000).
- [18] A. S. Kertes, *J. Inorg. Nucl. Chem.* **27**, 209 (1965).
- [19] S. Jurga, V. Macho, B. Huser, and H. W. Spiess, *Z. Phys. B: Condens. Matter* **84**, 43 (1991).
- [20] J. Stohrer, G. Gröbner, H. Reimer, K. Weisz, K. Mayer, and G. Kothe, *J. Chem. Phys.* **95**, 672 (1991).
- [21] Y. L. Wang, P. S. Belton, *Chem. Phys. Lett.* **325**, 33 (2000).
- [22] F. Bonetto, E. Anordo, and R. Kimmich *J. Chem. Phys.* **118**, 9037 (2003).
- [23] R. Y. Dong, *Nuclear Magnetic Resonance of Liquid Crystals* (Springer-Verlag, Berlin, 1997).
- [24] R. H. Acosta and D. J. Pusiol, *Phys. Rev. E* **63**, 011707 (2000).
- [25] A. Carvalho, P. J. Sebastião, A. C. Ribeiro, H. T. Nguyen, and M. Vilfan, *J. Chem. Phys.* **115**, 10 484 (2001), and references therein.
- [26] J. A. Marqusee, M. Warner, and K. A. Dill, *J. Chem. Phys.* **81**, 6404 (1984).
- [27] R. Blinc, M. Luzar, M. Vilfan, and M. Burgar, *J. Chem. Phys.* **63**, 3445 (1975).
- [28] M. Vilfan, G. Althoff, I. Vilfan, and G. Kothe, *Phys. Rev. E* **64**, 022902 (2001).
- [29] G. Althoff, O. Stauch, M. Vilfan, D. Frezzato, G. J. Moro, P. Hauser, R. Schubert, and G. Kothe, *J. Phys. Chem. B* **106**, 5517 (2002).
- [30] B. Halle, *Phys. Rev. E* **50**, R2415 (1994).
- [31] B. Halle and S. Gustafsson, *Phys. Rev. E* **56**, 690 (1997).
- [32] R. Kimmich and G. Voigt, *Chem. Phys. Lett.* **62**, 181 (1979).
- [33] S. Ljunggren and J. C. Eriksson, *J. Chem. Soc., Faraday Trans.* **87**, 153 (1991).
- [34] J. Charvolin and Y. Hendriks, *NMR of Liquid Crystals* (Reidel, Dordrecht, 1985).
- [35] S. Zumer and M. Vilfan, *J. Phys. (France)* **46**, 1763 (1985).
- [36] M. F. Brown, J. Seelig, and U. Häberlen, *J. Chem. Phys.* **70**, 5045 (1979).
- [37] W. Hübner and A. Blume, *J. Phys. Chem.* **94**, 7726 (1990).
- [38] J. Seelig, *Q. Rev. Biophys.* **10**, 353 (1977).
- [39] K. Weisz, G. Gröbner, C. Mayer, J. Stohrer, and G. Kothe, *Biochemistry* **31**, 1100 (1992).
- [40] D. Frezzato, G. Kothe, and G. Moro, *J. Phys. Chem. B* **105**, 1281 (2001).